$K^+ \to \pi^+ \nu\overline{\nu}$: first NA62 results

Radoslav Marchevski [a]
Department of experimental particle and astroparticle physics
Johannes Gutenberg University, Mainz, Germany

The decay $K^+ \to \pi^+ \nu\overline{\nu}$ with a very precisely predicted branching ratio of less than 10^{-10} is one of the best candidates to reveal indirect effects of new physics at the highest mass scales. The NA62 experiment at CERN SPS is designed to measure the branching ratio of the $K^+ \to \pi^+ \nu\overline{\nu}$ with a decay-in-flight technique, novel for this channel. NA62 has taken data firstly in 2016 with the aim to reach the SM sensitivity, it has then collected 10 times more statistics in 2017 and a similar amount of data is expected from the 2018 run. The preliminary result on $K^+ \to \pi^+ \nu\overline{\nu}$ from the full 2016 data set is presented and prospects for future developments reviewed.

[a] On behalf of the NA62 Collaboration: R. Aliberti, F. Ambrosino, R. Ammendola, B. Angelucci, A. Antonelli, G. Anzivino, R. Arcidiacono, M. Barbanera, A. Biagioni, L. Bician, C. Biino, A. Bizzeti, T. Blazek, B. Bloch-Devaux, V. Bonaiuto, M. Boretto, M. Bragadireanu, D. Britton, F. Brizioli, M.B. Brunetti, D. Bryman, F. Bucci, T. Capussela, A. Ceccucci, P. Cenci, V. Cerny, C. Cerri, B. Checcucci, A. Conovaloff, P. Cooper, E. Cortina Gil, M. Corvino, F. Costantini, A. Cotta Ramusino, D. Coward, G. D'Agostini, J. Dainton, P. Dalpiaz, H. Danielsson, N. De Simone, D. Di Filippo, L. Di Lella, N. Doble, B. Dobrich, F. Duval, V. Duk, J. Engelfried, T. Enik, N. Estrada-Tristan, V. Falaleev, R. Fantechi, V. Fascianelli, L. Federici, S. Fedotov, A. Filippi, M. Fiorini, J. Fry, J. Fu, A. Fucci, L. Fulton, E. Gamberini, L. Gatignon, G. Georgiev, S. Ghinescu, A. Gianoli, M. Giorgi, S. Giudici, F. Gonnella, E. Goudzovski, C. Graham, R. Guida, E. Gushchin, F. Hahn, H. Heath, T. Husek, O. Hutanu, D. Hutchcroft, L. Iacobuzio, E. Iacopini, E. Imbergamo, B. Jenninger, K. Kampf, V. Kekelidze, S. Kholodenko, G. Khoriauli, A. Khotyantsev, A. Kleimenova, A. Korotkova, M. Koval, V. Kozhuharov, Z. Kucerova, Y. Kudenko, J. Kunze, V. Kurochka, V.Kurshetsov, G. Lanfranchi, G. Lamanna, G. Latino, P. Laycock, C. Lazzeroni, M. Lenti, G. Lehmann Miotto, E. Leonardi, P. Lichard, L. Litov, R. Lollini, D. Lomidze, A. Lonardo, P. Lubrano, M. Lupi, N. Lurkin, D. Madigozhin, I. Mannelli, G. Mannocchi, A. Mapelli, F. Marchetto, R. Marchevski, S. Martellotti, P. Massarotti, K. Massri, E. Maurice, M. Medvedeva, A. Mefodev, E. Menichetti, E. Migliore, E. Minucci, M. Mirra, M. Misheva, N. Molokanova, M. Moulson, S. Movchan, M. Napolitano, I. Neri, F. Newson, A. Norton, M. Noy, T. Numao, V. Obraztsov, A. Ostankov, S. Padolski, R. Page, V. Palladino, C. Parkinson, E. Pedreschi, M. Pepe, M. Perrin-Terrin, L. Peruzzo, P. Petrov, F. Petrucci, R. Piandani, M. Piccini, J. Pinzino, I. Polenkevich, L. Pontisso, Yu. Potrebenikov, D. Protopopescu, M. Raggi, A. Romano, P. Rubin, G. Ruggiero, V. Ryjov, A. Salamon, C. Santoni, G. Saracino, F. Sargeni, V. Semenov, A. Sergi, A. Shaikhiev, S. Shkarovskiy, D. Soldi, V. Sougonyaev, M. Sozzi, T. Spadaro, F. Spinella, A. Sturgess, J. Swallow, S. Trilov, P. Valente, B. Velghe, S. Venditti, P. Vicini, R. Volpe, M. Vormstein, H. Wahl, R. Wanke, B. Wrona, O. Yushchenko, M. Zamkovsky, A. Zinchenko.

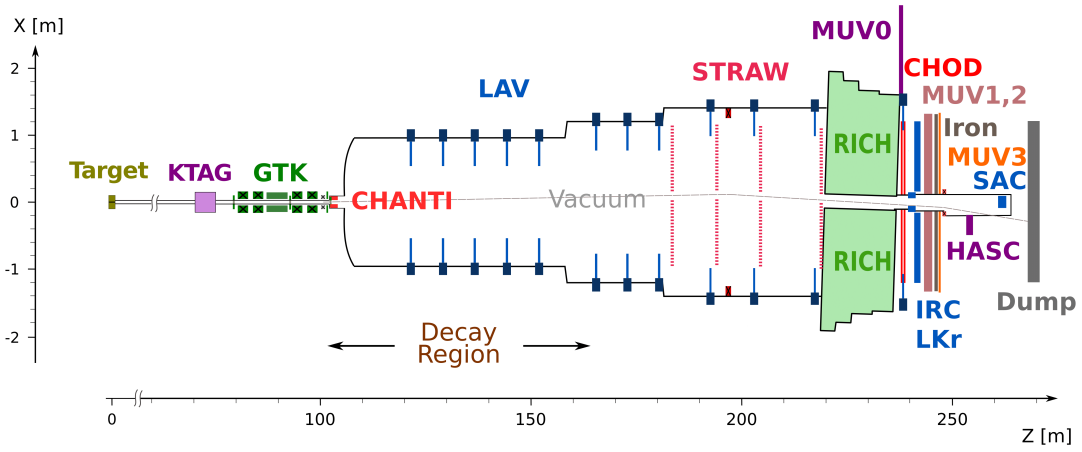

Figure 1: Schematic layout of the NA62 experiment in the xz plane

1 The $K^+ \to \pi^+\nu\bar{\nu}$ decay in the Standard Model

The $K^+ \to \pi^+\nu\bar{\nu}$, $(K_{\pi\nu\bar{\nu}})$ decay is a flavour changing neutral current process proceeding through box and electroweak penguin diagrams. The process is very rare, due to quadratic GIM mechanism and strong Cabibbo suppression. The dominant contribution comes from the short-distance physics of the top quark loop, with a small charm quark contribution and long-distance corrections. This makes the $K_{\pi\nu\bar{\nu}}$ very clean theoretically and sensitive to physics beyond the Standard Model (SM), probing the highest mass scales among the rare meson decays [1,2,3,4,5,6]. The SM prediction using elements of the Cabibbo-Kobayashi-Maskawa (CKM) matrix extracted from tree-level processes [7,8] is

$$BR(K^+ \to \pi\nu\bar{\nu}) = (8.4 \pm 1.0) \times 10^{-11}. \quad (1)$$

The knowledge of the external inputs dominate the uncertainties on the predictions. The experimental result from the BNL E949 collaboration [9]

$$BR(K^+ \to \pi\nu\bar{\nu}) = (17.3^{+11.5}_{-10.5}) \times 10^{-11}, \quad (2)$$

was obtained using stopped kaons. The branching ratio is $\sim 1\ \sigma$ away from the SM prediction, but the measurement was based on only few events and the experimental uncertainties are large.

2 NA62 beam and detector

The fixed target NA62 experiment aims at measuring the branching ratio of the $K_{\pi\nu\bar{\nu}}$ decay with a 10% precision. A sample of about 10^{13} kaon decays should be collected in few years of data-taking using the 400 GeV/c primary SPS proton beam. A maximum of 10% of background contamination is required, necessitating a background rejection factor of the order of 10^{12}. The beam impinges on a beryllium target producing secondary particles, of which the kaon component is 6%. A 100 m long beam line selects, collimates, focuses and transports charged particles of (75.0±0.8) GeV/c momentum to the evacuated fiducial decay volume.

The NA62 experimental apparatus is shown in Figure 1. The KTAG is a differential Cherenkov detector filled with N_2 placed in the beam to identify and timestamp kaons. It is followed by the Gigatracker (GTK) detector, composed of three silicon pixel stations of 6×3 cm^2 surface exposed to the full 750 MHz beam rate. The GTK is used to timestamp and measure the momentum of the beam particles before entering the vacuum region downstream. The CHANTI detector, placed after the Gigatracker, tags hadronic beam-detector interactions in the last GTK station. Downstream, the magnetic spectrometer made of four straw chambers and a

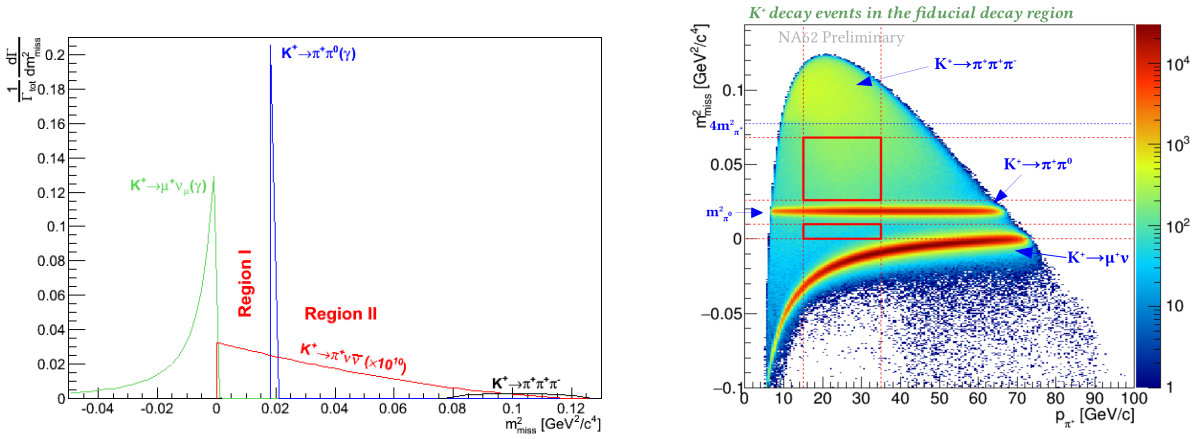

Figure 2: Left: m^2_{miss} shapes for signal and backgrounds of the main K^+ decay modes: the backgrounds are normalized according to their branching ratio; the signal is multiplied by a factor 10^{10} Right: Distribution of m^2_{miss} as a function of track momentum for events selected on minimum bias data; The bands corresponding to $K^+ \to \pi^+\pi^0$ and $K^+ \to \mu^+\nu_\mu$ decays are clearly visible; the signal regions (red box) are drawn for reference.

dipole magnet between the second and third chamber is used to measure the momentum of the charged K^+ decay particles. A 17 m long RICH counter filled with neon gas is used to separate π^+, μ^+ and e^+. The time of charged particles is measured both with the RICH and with an array of scintillators (CHOD) located downstream of the RICH. Two hadronic calorimeters (MUV1 and MUV2) and a fast scintillator array (MUV3) provide further separation between π^+ and μ^+. A set of photons vetoes (LAVs, LKr, IRC, SAC) hermetically cover angles up to 50 mrad to reject extra electromagnetic activity. A detailed description of the apparatus and its performances in 2015 can be found in the NA62 beam and detector paper [10].

3 The $K^+ \to \pi^+\nu\bar{\nu}$ analysis

The analysis of the complete 2016 data set is presented here, corresponding to a total number of kaon decays in the fiducial decay region $N_K = 1.21(2) \times 10^{11}$. The $K_{\pi\nu\bar{\nu}}$ decay signature is one track in the initial and final state with two missing neutrinos. The main kinematic variable is $m^2_{miss} \equiv (p_K - p_{\pi^+})^2$, where p_K and p_{π^+} are the 4-momenta of the K^+ and π^+ respectively. The theoretical shape of the main K^+ background decay modes are compared to the $K_{\pi\nu\bar{\nu}}$ in Figure 2-left.

The analysis is performed in two separate regions: Region 1 (R1) between the $K^+ \to \mu^+\nu_\mu\,(K_{\mu\nu})$ and $K^+ \to \pi^+\pi^0\,(K_{\pi\pi})$ contribution and Region 2 (R2) between $K_{\pi\pi}$ and $K^+ \to \pi^+\pi^+\pi^-\,(K_{\pi\pi\pi})$ contribution. The main backgrounds entering those regions are $K_{\mu\nu}$ and $K_{\pi\pi}$ decays through non-gaussian resolution and radiative tails; $K_{\pi\pi\pi}$ through non-gaussian resolution; $K^+ \to \pi^+\pi^-e^+\nu_e\,(K_{e4})$ and $K^+ \to l^+\pi^0\nu_l\,(K_{l3})$ decays with neutrinos in the final state ($l = \mu,\, e$); upstream background consisting of K^+ decays upstream of the GTK3 station and inelastic beam-detector interactions. Each of the background processes requires different rejection procedure depending on its kinematics and type of charged particle in the final state.

Events with single track topology are selected using the downstream detectors STRAW, CHOD and RICH. The track must have a matching pair of slabs in the CHOD and a reconstructed ring in the RICH, where the time is measured with 100 ps resolution. The downstream track is then associated to an in-time kaon in the KTAG detector. The K^+ track is then reconstructed and time-stamped in the GTK detector. A kaon decay vertex is created at the intersection point of the GTK and STRAW tracks. The kaon decays within a 50 m fiducial region beginning 10 m downstream to the last GTK station (GTK3) are selected (Figure 2-right).

Source	δSES (10^{-10})
Random veto	± 0.17
Definition of $\pi^+\pi^0$ region	± 0.10
$A_{\pi\nu\nu}$	± 0.09
N_K	± 0.05
Trigger efficiency	± 0.04
Extra activity	± 0.02
Pileup simulation	± 0.02
Momentum spectrum	± 0.01
Total	± 0.24

Table 1: Sources of systematic uncertainties to SES. See text for the definition of the various sources.

The π^+ tracks are identified by the calorimeters and the RICH counter providing 10^8 muon suppression for 64% π^+ efficiency. The performances are measured on kinematically selected $K_{\pi\pi}$ and $K_{\mu\nu}$ decays on control-trigger data.

Events passing the π^+ identification criteria are mainly $K_{\pi\pi}$ decays, which are further suppressed by rejecting in-time coincidences between the π^+ and energy deposits in the electromagnetic calorimeters LKr, LAVs, SAC, IRC. The resulting π^0 suppression is 3×10^{-8}, as measured from minimum bias and $K_{\pi\nu\overline{\nu}}$-trigger streams before and after γ rejection, respectively.

Signal region definitions are driven by the $m^2_{miss}(STRAW, GTK)$ resolution $\sigma(m^2_{miss}) = 1 \times 10^{-3}$ GeV$^2/c^4$. To protect against kinematic misreconstruction additional constraints are imposed on the $m^2_{miss}(RICH, GTK)$ computed by replacing the STRAW momentum with that measured by the RICH under a π^+ mass hypothesis and $m^2_{miss}(STRAW, Beam)$ computed by using nominal K^+ momentum. The total $K_{\pi\nu\overline{\nu}}$ acceptance after the complete selection and signal region definition is 4%, divided between R1(1%) and R2(3%).

The probability of the $K_{\mu\nu}(K_{\pi\pi})$ decays to enter the signal regions defined by the three m^2_{miss} is $3 \times 10^{-4}(1 \times 10^{-3})$. This kinematic suppression factor is used for the background estimation and is measured using $K_{\mu\nu}(K_{\pi\pi})$ decays selected with $\pi\nu\overline{\nu}$-like selection on a control-trigger data sample.

The single event sensitivity for a SM $K_{\pi\nu\overline{\nu}}$ decay is $SES = (3.15 \pm 0.01_{stat} \pm 0.24_{syst}) \times 10^{-10}$, dominated by systematic uncertainty. Summary of the systematic uncertainties on the SES is presented in Table 1. The uncertainty is dominated by: random veto losses induced by the π^0 rejection procedure; stability of the SES estimation when varying the $\pi^+\pi^0$ normalization region; simulation of the π^+ losses due to interactions in the detector material upstream of the hodoscopes.

The behaviour of the $K^+ \to \pi^+\pi^0(\gamma)$ and $K^+ \to \mu^+\nu_\mu(\gamma)$ background decays is shown in Figure 3 as a function of the P_{π^+} momentum and compared to the signal expectation. The $K_{\pi\pi(\gamma)}\,(K_{\mu\nu})$ background is dominating at low(high) P_{π^+}. The shape of the other background processes can't be studied with the 2016 data set because the limited statistics. A MC simulation of 400 million generated $K^+ \to \pi^+\pi^- e^+\nu_e\,(K_{e4})$ decays is used to estimate the expected background. The simulation is validated on data using 5 independent samples. The precision of the K_{e4} background estimation is limited by the size of the MC sample. The upstream background is estimated using a data driven method. The method is statistically limited, reflected in the large uncertainty dominating the overall background estimation.

Process	Expected events in R1+R2
$K^+ \to \pi^+\nu\bar{\nu}$ (SM)	$0.267 \pm 0.001_{stat} \pm 0.020_{syst} \pm 0.032_{ext}$
$K^+ \to \pi^+\pi^0(\gamma)$ IB	$0.064 \pm 0.007_{stat} \pm 0.006_{syst}$
$K^+ \to \mu^+\nu(\gamma)$ IB	$0.020 \pm 0.003_{stat} \pm 0.003_{syst}$
$K^+ \to \pi^+\pi^-e^+\nu$	$0.018^{+0.024}_{-0.017}\vert_{stat} \pm 0.009_{syst}$
$K^+ \to \pi^+\pi^+\pi^-$	$0.002 \pm 0.001_{stat} \pm 0.002_{syst}$
Upstream Background	$0.050^{+0.090}_{-0.030}\vert_{stat}$
Total Background	$0.15 \pm 0.09_{stat} \pm 0.01_{syst}$

Table 2: Summary of the expected number of signal and background events in R1 and R2 after the $K_{\pi\nu\bar{\nu}}$ analysis is applied on the complete 2016 data set.

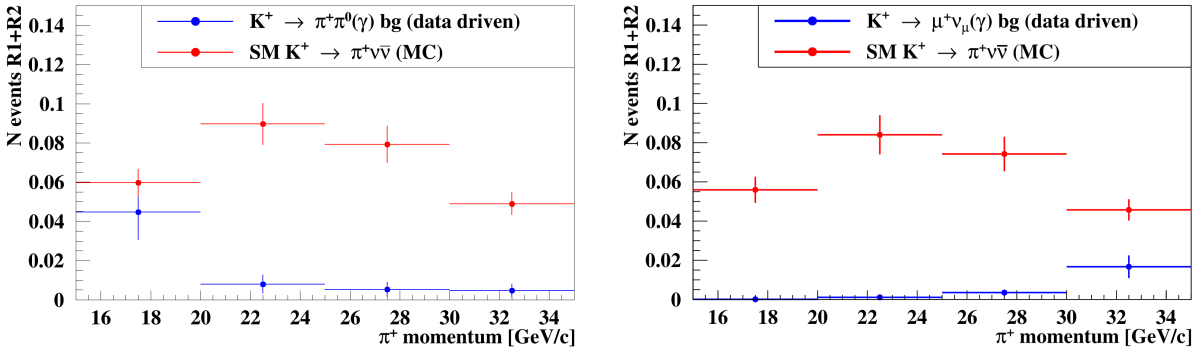

Figure 3: Left: Expected number of $K^+ \to \pi^+\pi^0(\gamma)$ background events in R1 and R2 in bins of P_{π^+} compared to the expected number of SM $K^+ \to \pi^+\nu\bar{\nu}$ events. Right: Same as left plot, but for the $K^+ \to \mu^+\nu_\mu(\gamma)$ background. Uncertainties on the background estimations are statistical only, while on expected signal are mostly systematic.

4 Results

One event is found in R2 after un-blinding the signal regions. The $K_{\pi\nu\bar{\nu}}$ candidate event (Figure 4-left) has 15.3 GeV/c momentum and is perfectly consistent with a π^+ track in the RICH detector (Figure 4-right). Upper limit on the branching ratio of the $K^+ \to \pi^+\nu\bar{\nu}$ decay are obtained using the CL$_s$ method [11]:

$$BR(K^+ \to \pi^+\nu\bar{\nu}) < 14 \times 10^{-10} \text{ @ 95\% CL} \quad \text{observed limit}$$
$$BR(K^+ \to \pi^+\nu\bar{\nu}) < 10 \times 10^{-10} \text{ @ 95\% CL} \quad \text{expected limit.}$$

Alternatively the Rolke-Lopez method [12] is used, assuming a Poisson process in the presence of background with a gaussian uncertainty. The results are in agreement with the CL$_s$ treatment.

A measurement of the branching ratio at 68% CL is also computed after subtracting the expected background

$$BR(K^+ \to \pi^+\nu\bar{\nu}) = 2.8^{+4.4}_{-2.3} \times 10^{-10} \text{ @ 68\% CL.}$$

No statistically significant signal observation can be claimed, therefore the branching ratio is shown only for comparison with the result obtained by the BNL E949 collaboration $BR(K^+ \to \pi^+\nu\bar{\nu}) = 1.73^{+1.15}_{-1.05} \times 10^{-10}$ @ 68% CL [9] and with the Standard Model prediction $BR(K^+ \to \pi^+\nu\bar{\nu}) = (0.84 \pm 0.10) \times 10^{-10}$. Our result is in agreement with both the SM prediction and previous measurements.

The analysis of the 2016 data set proves that the decay-in-flight technique of NA62 to study $K^+ \to \pi^+\nu\bar{\nu}$ works. The $K^+ \to \pi^+\nu\bar{\nu}$ analysis of the 2017 data is ongoing. Improvements

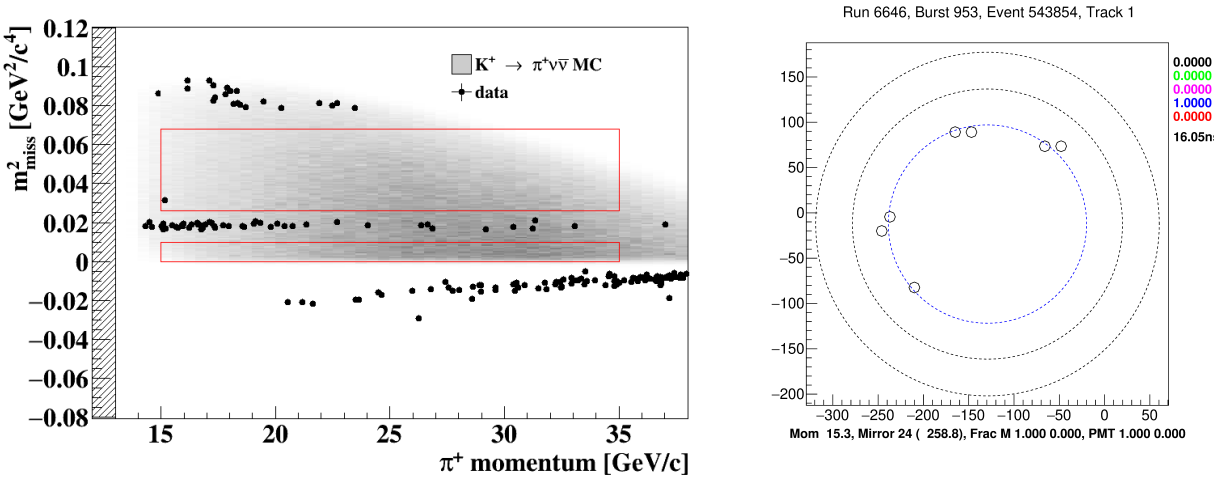

Figure 4: Left: m^2_{miss} as a function of P_{π^+} (dots) after the complete $K^+ \to \pi^+\nu\overline{\nu}$ selection is applied, but the cuts on m^2_{miss} and P_{π^+}. The gray area corresponds to the distribution of $K^+ \to \pi^+\nu\overline{\nu}$ MC events. The red lines correspond to the two signal regions. The event observed in R2 is shown. Right: Position of the hits in the RICH forming the ring associated to the π^+ track in the observed event in R2, given by the RICH event display. The circles illustrate the positron, muon and pion hypothesis, showing a perfect agreement with the pion hypothesis (the innermost ring).

at both hardware and analysis level are foreseen to reduce the background and improve signal efficiency. Considering the statistics collected in 2017 and expected in 2018, NA62 should observe about 20 SM $K^+ \to \pi^+\nu\overline{\nu}$ events with the complete data set.

References

1. M. Blanke, A. J. Buras, B. Duiling, K. Gemmler , S. Gori, *JHEP* **903**, 108 (2009)
2. A. J. Buras, D. Buttazzo, R. Knegjens, *JHEP* **1511**, 166 (2015)
3. T. Blazek, P. Matak, *Int. J. Mod. Phys.* A **29.no.27**, 1450162 (2014)
4. Isidori et al., *JHEP* **0608**, 064 (2006)
5. M. Blanke, A. J. Buras, S. Recksiegel, *Eur. Phys. J.* C **76.no.4**, 182 (2016)
6. J. Isidori, M. Bordone, D. Buttazzo, J. Monnard, *Eur. Phys. J.* C **77**, 618 (2017)
7. A. J. Buras, D.Buttazzo, K.Girrbach-Noe, R. Knegjens, *JHEP* **11**, 033 (2015)
8. J. Brod, M. Gorbahn, E. Stammou, *Phys. Rev.* D **83**, 034030 (2011)
9. The E949 Collaboration, *Phys. Rev.* D **79**, 092004 (2009)
10. The NA62 Collaboration *JINST* **12**, P05025 (2017)
11. A. L. Read, *J. Phys.* G **28**, 10 (2002)
12. W.A. Rolke, A.M. Lopez, *Nucl. Instrum. Methods* A **506**, 250 (2003)